Polymer 50 (2009) 5733–5743

Contents lists available at ScienceDirect

Polymer

journal homepage: www.elsevier.com/locate/polymer

Interface/morphology relationships in polymer blends with thermoplastic starch

Aurélie Taguet [a], Michel A. Huneault [b], Basil D. Favis [a,*]

[a] CREPEC, Department of Chemical Engineering, Ecole Polytechnique de Montréal, 2900 Edouard Montpetit, P.O. 6079, Station Centre-Ville, Montréal, QC, H3C 3A7, Canada
[b] Industrial Materials Institute – National Research Council Canada, 75 Boul. de Mortagne, Boucherville, Québec, J4B 6Y4, Canada

ARTICLE INFO

Article history:
Received 24 April 2009
Received in revised form
17 September 2009
Accepted 18 September 2009
Available online 24 September 2009

Keywords:
Thermoplastic starch
Polymer blends
HDPE-*g*-MA copolymer

ABSTRACT

In this paper, the interface/morphology relationship in polyethylene/TPS blends prepared by a one-step extrusion process is examined in detail. Emulsification curves tracking the change in phase size with added quantity of PE-g-MA copolymer are used to identify the critical concentration required for saturation of the interface as well as to estimate the areal density of grafted copolymer chains at the interface. The level of glycerol content in the TPS is shown to lead to different emulsification behaviors. Dynamic mechanical analysis clearly shows a partial miscibility between glycerol and starch in the TPS with glycerol-rich and starch-rich peaks being clearly identified. This phase separation is more evident in the case of high glycerol levels in the TPS (>24% glycerol). Furthermore, the glycerol-rich peak decreases in intensity with added PE-g-MA graft copolymer. At high glycerol contents (>24% glycerol) in the TPS, a 20% thermoplastic starch-based binary blend with polyethylene can reach an elongation at break value as high as 200%. When also modified at the appropriate level with a PE-g-MA copolymer, this elongation at break further increases to 600%. However, at lower glycerol contents, the elongation at break is comparatively low at 20–50% even after the addition of PE-g-MA copolymer. We explain these results through a proposed double mechanism of interfacial modification between the HDPE matrix and the TPS dispersed phase. Under dynamic melt-mixing conditions, it is suggested that a small portion of the low molecular weight glycerol-rich phase tends to migrate to the HDPE-TPS interface as predicted by Harkins spreading theory. Once at the interface, this glycerol-rich outer layer is readily deformed by an applied stress and this stress is then transferred to the starch-rich phase due to their mutual partial miscibility. Added PE-g-MA copolymer initially reacts with the glycerol-rich outer layer but if the level of copolymer is high enough, it then reacts with the starch-rich phase via a classic interfacial modification protocol. Also, both the elongation at break and impact properties dramatically increase at a copolymer level associated with interfacial saturation. The above mechanism effectively explains all the emulsification and mechanical property observations.

1. Introduction

Starch is a natural carbohydrate storage material accumulated in plants in the form of granules and is a biodegradable annually renewable resource of low cost. It is composed of linear polysaccharide molecules (amylose) and branched molecules (amylopectin). Native starch granules swell when they absorb water through hydrogen bonding with their free hydroxyl groups. When these swollen starch granules are heated, gelatinization occurs [1]. The addition of a plasticizer such as glycerol combined with heating and high shear can further improve the ductility of gelatinized starch and the obtained plasticized starch is known as thermoplastic starch (TPS). Unfortunately, thermoplastic starch is a very hydrophilic material with limited performance.

The hydrophilicity of thermoplastic starch can be overcome by melt blending with hydrophobic polymers, such as polyethylene. PE and TPS form immiscible blends due to the high interfacial tension between the non-polar PE and the highly polar TPS [2,3]. The mixing of conventional polymers with native unplasticized starch blends always leads to brittle materials [2,4,5]. In that case the starch component behaves as a solid filler. The first investigation on thermoplastic starch/polyethylene blends was carried out by St Pierre et al. [6] who demonstrated that dispersed phase/matrix morphology control protocols could be applied to this blend. In a later work, Rodriguez et al. [7–10] developed an effective one-step melt processing technique and controlled the level of continuity of the TPS phase. This resulted in exceptional properties for the PE/TPS blends. This process was used to generate highly

* Corresponding author. Tel.: +1 514 340 4711x4527; fax: +1 514 340 4159.
E-mail address: basil.favis@polymtl.ca (B.D. Favis).

0032-3861/$ – see front matter © 2009 Elsevier Ltd. All rights reserved.
doi:10.1016/j.polymer.2009.09.055

elongated morphological structures [9]. With this approach it was possible to achieve blends where the TPS morphology could be effectively controlled, yielding a wide range of sophisticated morphological states. Rodriguez et al. [8,11] succeeded in maintaining 96% of the elongation at break and 100% of the modulus of LDPE with a 71:29 HDPE/TPS blend that contained 36% of glycerol in the TPS phase. Moreover, this particular blend demonstrated very low levels of sensitivity to moisture and an absence of interfacial voiding.

In order to improve the compatibility of the blends, TPS can be blended with PE using a compatibilizer. The most common compatibilizers are poly(ethylene-*co*-glycidyl methacrylate) (PEGMA) [12,13], poly(ethylene-*co*-acrylic acid) (EAA) [14], poly(ethylene-*co*-vinyl alcohol) (EVOH) [15], poly(ethylene-*g*-maleic anhydride) (PE-*g*-MA) copolymers [16,17], and more recently Sailaja et al. used poly(LDPE-*g*- dibutyl maleate) copolymer [18].

In the compatibilization of LDPE/TPS blends with PE-*g*-MA copolymers, the maleic anhydride group reacts with the hydroxyl groups of starch while the PE chains interact with the PE matrix [19]. This allows the PE-g-MA copolymer to place itself at the interface of PE/TPS during melt blending. The improved adhesion between phases leads to better mechanical properties; Sailaja et al. [12,17] showed a reduction of the modulus and the improvement of the elongation at break by adding LDPE-*g*-MA or PEGMA copolymers to PE/TPS blends. They attributed the drop of the modulus to the increase in the chain flexibility of starch after addition of compatibilizer. PE-*g*-MA [5], PEGMA [12] and EVOH [15] copolymers increase the impact strength of HDPE/TPS, LDPE/TPS and LDPE/TPS blends, respectively. Compatibilized PE/TPS blends exhibit ductile fracture with large plastic deformation [12]. With only 10% of PEGMA added to a 20TPS/80LDPE blend, Sailaja et al. [12] found that a quasi-cleavage ductile fracture came from a high number of microcracks that originated from one of the elongated voids. More recently, Wang et al. [20] extruded blends of LLDPE/TPS in the presence of citric acid (CA), and the acidity of CA was propitious to improve the plasticization of starch and dispersion between LLDPE and TPS. Hence they observed an increase of the mechanical properties in the presence of CA. In a study on PLA/TPS blends, Huneault et al. [21] showed that a significant increase in elongation at break for PLA/TPS blends could be achieved by grafting maleic anhydride unto PLA and then subsequently blending the grafted PLA with TPS. They attributed this rise in mechanical properties to a reduced interfacial tension between PLA and TPS after compatibilization, as evidenced by a significant reduction in the phase size of dispersed TPS domains. Although the above authors have shown the potential of compatibilization to improve the mechanical properties of thermoplastic starch blends, few papers have examined the detailed morphology/interface relationship in polymer blends with thermoplastic starch.

For polymer blends, the modification of the interface serves to reduce the interfacial tension between the major components and results in a significant diminution in the dispersed phase particle size. Taylor's theory [22,23] predicts a direct relationship between the interfacial tension and size of the dispersed phase. The emulsification curve which tracks dispersed phase particle size with interfacial modifier concentration has been shown to be a powerful technique to elucidate fundamental information related to the interface such as the critical concentration for interfacial saturation and also the area occupied by the copolymer at the interface [24]. The stable location of the copolymer at the interface essentially depends on its molecular weight [25,26], architecture, chemical composition [27], as well as the number of blocks [28].

To date, very little detailed information on interface/morphology relationships has been published with respect to blends with biopolymers. The investigation of blends with thermoplastic starch provides a particularly complex system due to the high concentrations of low molecular plasticizer present in the system. Understanding the behaviour at the interface between the TPS dispersed phase and the matrix is essential since it governs the morphology of the blend and also its physical and mechanical properties.

The objective of this paper is to examine the fundamental interface/morphology relationships in polyethylene/TPS blends prepared by a one-step extrusion process. The detailed dependence of the morphology on interfacial modifier, the areal density of modifier at the interface, the critical concentration required for saturation of the interface as well as dynamic and static mechanical properties will be investigated. A qualitative model for the interface of this blend system will be advanced.

2. Experimental section

2.1. Material

The high density polyethylene (HDPE) was supplied by Nova Chemicals, and was a Sclair® HDPE2710. The native wheat starch (Supergell 1203-C) and the glycerol were obtained from ADM and Labmat, respectively. The wheat starch was composed of 25% amylose and 75% amylopectin. The glycerol was pure at 99.5% and contained 0.5% water. (2-dodecen-1-yl)succinic anhydride was purchased form Aldrich.

The PE copolymer grafted with maleic anhydride (PE-*g*-MA) had a MA concentration equal to 3.9% as measured by elemental analysis. Some properties of these materials are shown in Table 1. The density of the TPS was estimated by PVT studies in this laboratory to be 1.4. The density of polyethylene was obtained from the supplier.

Starch, glycerol and water were mixed to form the suspensions used in the melt blending experiments. The water, starch and glycerol contents of the different suspensions are mentioned in Table 2.

2.2. Blend preparation

Starch granules were gelatinized, plasticized with glycerol and water and blended with HDPE and compatibilizer in a one-step extrusion process. Blends were prepared containing 20 wt% of TPS and 80 wt% of HDPE. The compatibilizer was added with the HDPE, at various rates. All compatibilizer concentrations are based on the TPS content.

The processing of the polyethylene/thermoplastic starch blends was based on a process developed previously in this laboratory [7,8,10]. More detailed information related to the process is given in those articles. The extrusion system was composed of a single-screw extruder (SSE) connected midway to a co-rotating twin-screw extruder (TSE). A starch/glycerol/water suspension was fed in the first zone of the TSE. Native starch was gelatinized and plasticized and volatiles were extracted in the first part of the TSE. Molten HDPE and copolymer (T = 160 °C) were fed from the SSE to

Table 1
Properties of the materials.

Materials	Density (g/cm^3)	Melt flow rate (at 190 °C)	M_n; M_w (g/mol)
HDPE	0.951	17 g/10 min	-
Wheat starch	1.4 (specific gravity)	-	-
Glycerol	1.26	-	92.09
HDPE-*g*-MA copolymer	0.95	12 g/10 min	31200; 112500

Table 2
Composition of the starch suspensions.

Code[a]	Wt% water	Wt% glycerol	Wt% starch
TPS24	32.6	16.6	50.8
TPS28	29.5	20.2	50.3
TPS36	23.4	28.1	48.5
TPS40	20.4	32.4	47.2

[a] The exact glycerol content for each of the TPS samples shown in the Table can be found in the Experimental.

midway on the TSE. TPS, HDPE and copolymer were then mixed in the latter part of the TSE. The TSE screw speed was 150 rpm for all blends. A three-hole strand die (diameter 3 mm) was used and strands were water cooled, followed by air cooling and then pelletized.

Note that the TPS prepared from suspensions containing 16.6, 20.2, 28.1 and 32.4 wt% glycerol, are designated in Table 2 as TPS 24, 28, 36 and TPS 40 throughout this work. The 24 in TPS 24 corresponds to the weight of glycerol divided by the weight of glycerol and starch (including ambient water in the as-received starch, but not including any added excess water). After plasticization of the starch, water was removed using a venting process. Under such conditions, virtually all of the water was removed (including native water within the as-received starch). As such, the actual final glycerol content of the TPS after extrusion is 26, 30, 38 and 42% (based on the weight of thermoplastic starch) for TPS 24, 28, 36 and TPS 40 respectively.

For clarity, a conventional code is given to all samples: for example, 20TPS36C2 refers to a blend containing 20 wt% of TPS36 as dispersed phase and 2 wt% of compatibilizer (based on TPS).

2.3. Scanning electron microscopy and image analysis

Samples were cryogenically fractured parallel and perpendicular to the machine direction and microtomed at −150 °C under liquid nitrogen using a glass knife to create a plane face. The instrument was a Leica-Jung RM 2165 equipped with a Leica LN 21 type cryochamber. TPS was extracted at room temperature with 6 N HCl for 2 h. The samples were then washed with water, dried under air and coated with a gold-palladium alloy. The observations were carried out using a Jeol JSM 840 Scanning Electron Microscope (SEM) operated at a voltage of 5 kV.

In order to plot the emulsification curves, the SEM micrographs of the samples cut perpendicular to the machine direction were analyzed by a semiautomatic method of image analysis, consisting of a digitizing table and in-house developed software, described elsewhere [29]. For each sample, between 300 and 500 diameter measurements were made, from which the volume average diameter d_v, surface average diameter d_s and number average diameter d_n were obtained. A correction procedure developed by Saltikov was applied to the diameters determined from micrographs [30]. This was done to take into account the polydispersity in particle size, and the fact that the knife rarely cuts the dispersed phase particles at the equator. In all our papers using emulsification curves, we have estimated the critical concentration for interfacial saturation by tracing a straight line through the plateau value data and then observing the lower limiting modifier concentration which results in a positive deviation from that straight line behavior. It should be noted that although sample replication was not carried out for every data point, each point in the emulsification curve is a separately prepared mixture. Hence the points in the plateau region of the emulsification curves give essentially the variation. The extent of variation has been reported extensively by us in morphology and image analysis of polymer blend systems in previous work [24,26–28,31] and does not exceed plus or minus 10% of the reported value.

2.4. Fourier transform infrared spectroscopy (FTIR)

FTIR spectroscopy was used to investigate the reaction between the glycerol and anhydride. Glycerol and (2-dodecen-1-yl) succinic anhydride were introduced in stoichiometric quantities with ethanol (solvent) in a round-bottom flask equipped with a condenser. Note that the (2-dodecen-1-yl) succinic anhydride was only used for the FTIR study and is not a maleic anhydride. After 24 h of reaction at 80 °C, the ethanol was evaporated and the obtained product was analyzed in the FTIR, with the starting materials. A Magma 860 IR from Nicolet equipped with an Attenuated Total Reflectance (ATR) was used to perform the spectra in transmittance versus wavenumber.

2.5. Dynamic mechanical thermal analysis (DMTA)

Dynamic thermal properties were measured using a TA dynamic mechanical analyzer (TA Instruments Model DMA 2980). The temperature was increased from −100 to 100 °C, with a heating rate of 3 °C/min. The frequency was 1 Hz, and the oscillation amplitude was 30 μm. The measurements were carried out using the dual cantilever clamp mode on injection molded samples of size $41.24 \times 9.66 \times 3.05$ mm^3.

2.6. Izod impact resistance

After compounding, samples were injection molded into rectangular bars with a Sumitomo SE50S injection machine. The dimension of the unnotched specimens was $62.10 \times 12.40 \times 4.62$ mm^3. Samples were conditioned for 48 h at 23 °C and 50% humidity. Then, unnotched specimen measurements were performed with the Resil 25 Izod impact tester from Ceast according to ASTM 4812. Seven specimens were tested and their average value was reported. Only the energy for 20TPS24 and 20TPS28 blends are reported because 20TPS36 and 20TPS40 were too ductile and did not break even when submitted to the heaviest pendulum.

2.7. Tensile properties

After extrusion, samples were injection molded into dumbbell-shaped specimens of dimensions: $57.00 \times 9.70 \times 3.05$ mm^3. Samples were conditioned for 48 h at 23 °C and 50% humidity. Tensile measurements were performed according to ASTM D638 with an Instron 4400R universal testing machine at a crosshead speed of 50 mm/min. The elongation at break, ϵ_b (expressed in %), was determined from the stress-strain curves. At least ten specimens of each sample were tested and their average value was reported with error bars including the minimum and the maximum obtained values of elongation.

3. Results and discussion

3.1. Emulsification

Fig. 1 shows typical micrographs of these blends both before and after compatibilization. Both transverse and machine direction photos are shown illustrating the isotropic character of these mixtures. The volume-average dispersed phase diameters for blends without interfacial modifier and as a function of glycerol content are plotted in Fig. 2. The d_v of the TPS24 blend is dramatically higher than that of higher glycerol content blends. Low glycerol contents (24%) are insufficient to fully destructurize and plasticize the native starch and in that case the starch phase size is similar to the native dry granular starch. Moreover, as shown by Rodriguez et al.[8], the higher the glycerol amount, the lower the

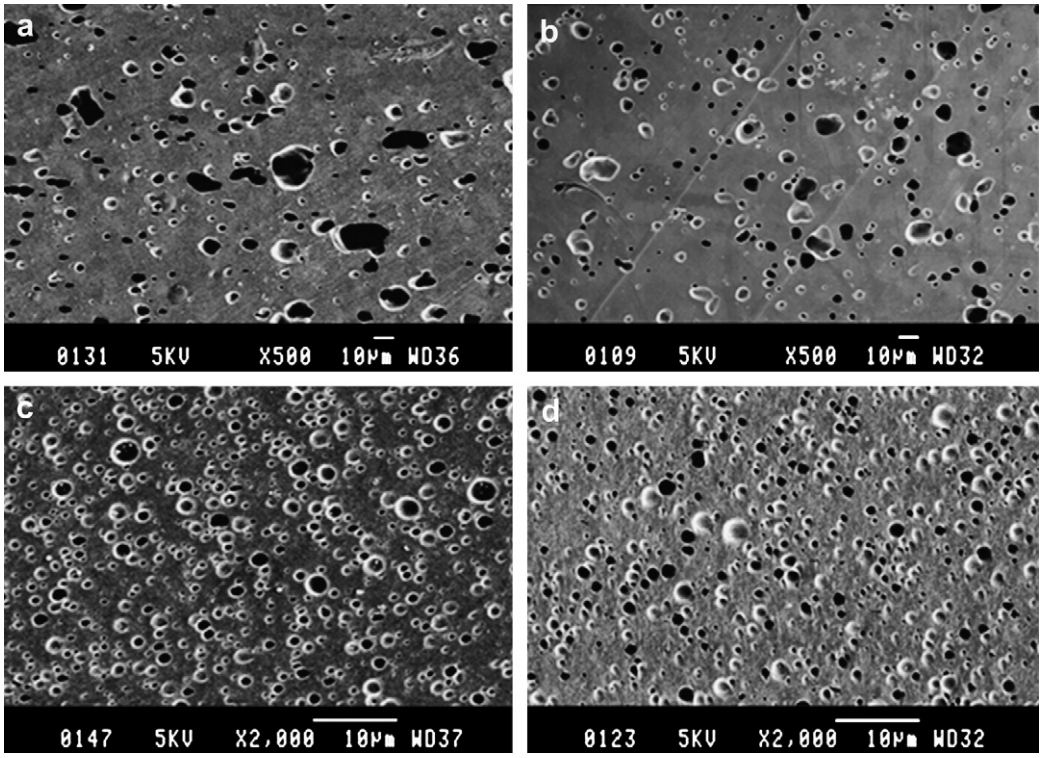

Fig. 1. SEM images (after extraction of the TPS phase) of a) 20TPS28C0 in the machine direction, b) 20TPS28C0 in the transverse direction, c) 20TPS28C9 in the machine direction and d) 20TPS28C9 in the transverse direction.

viscosity of the TPS. In the case of the 20TPS24C0 blend, both low plasticization and consequently a high viscosity of TPS are responsible for the high volume average diameter (30.5 μm) of the TPS dispersed phase while for the case of 20TPS40C0, the phase size is 2.9 μm. Fig. 2 suggests that the plasticization threshold is close to 28 wt% of glycerol. Rodriguez [8] found that 30% glycerol is required to effectively plasticize starch and that blend morphology control protocols require a very high level of plasticization.

In order to examine the case of interfacially modified blends, a maleic anhydride grafted copolymer was added with the HDPE. The role of an interfacial modifier, such as PE-*g*-MA copolymer is to decrease the interfacial tension between both immiscible phases,

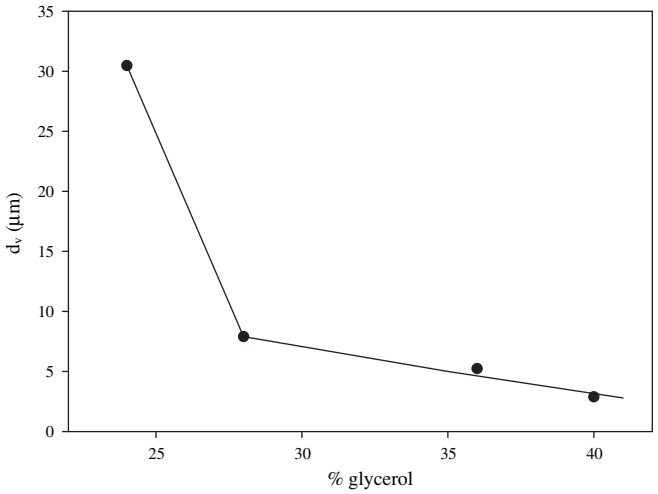

Fig. 2. Volume-average diameter of TPS phase versus the wt% of glycerol for unmodified blends.

and hence to decrease the dispersed phase size [22,23,31,32]. This decreasing of the interfacial tension is due to the reaction of esterification between the maleic anhydride of the PE-*g*-MA copolymer and the OH of the starch [16,19,33,34].

Equilibrium dispersed phase morphologies are obtained through a combination of viscous forces tending to deform the droplet and interfacial tension tending to keep the drop intact. This, counterbalanced with coalescence, leads to an equilibrium phase size. The twin-screw extruder is an extremely powerful mixing device and we have shown in previous work [35] that, once the systems are melted, the morphology is established very quickly. In the presence of an interfacial modifier, the morphology is established even more readily.

Emulsification curves are usually characterized by a rapid drop in the dispersed phase particle size, as well as a drop in the particle size distribution, at low concentration of interfacial modifier. This is then followed by a leveling off to a constant phase size value at a certain concentration of compatibilizer. The emulsification curves of blends of 20TPS28 can be seen in Fig. 3a, where the particle size drops and the plateau phase size at a critical concentration of copolymer are evident. The volume average, surface average and number average phase size diameters are shown. Fig. 3b shows that the TPS phase size, for both uncompatibilized and compatibilized 20TPS28 blends, follows a log-normal distribution. It is clear that the TPS particle sizes are significantly lower for the 13%- PE-*g*-MA copolymer compatibilized blend as compared to the uncompatibilized one.

The morphology data were collected for blends containing 24, 28, 36 and 40 wt% glycerol. In Fig. 4, only the d_v is plotted since it is known to best indicate the point of interfacial saturation. The amount of glycerol has a dramatic influence on the behaviour of the emulsification curves. Also, as mentioned previously, the higher the glycerol amount, the lower is the TPS particle size. When the copolymer is added at low concentration to 20TPS24, 20TPS28 and

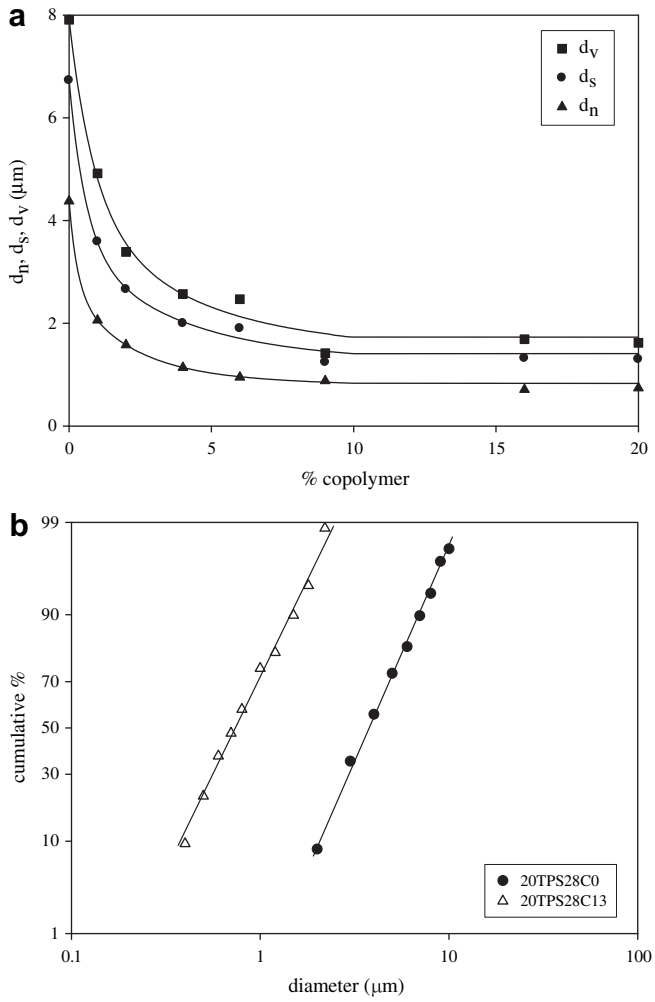

Fig. 3. Log-normal distribution of the TPS phase size in a 20% TPS28 blend containing 0% (●) and 13% (r) of copolymer (copolymer content is based on the dispersed phase).

20TPS36 blends (Fig. 4a, b and c), it migrates to the interface to reduce the interaction between the two immiscible polymers. The main consequences on the emulsification curves are first a decrease in the average diameters (note that the initial decrease in phase size is less pronounced for 20TPS36). Afterwards, the leveling off of dispersed phase size observed at higher copolymer concentration is an indication of interfacial saturation by the copolymer. This concentration is known as the critical concentration or saturation concentration for emulsification, and is noted as C_{crit} [24,36]. Above this copolymer concentration, there is no further decrease in the particle size and excess copolymer migrates to the matrix in the form of micelles [25,37–39]. For the blend containing 40 wt% glycerol, the behaviour of the emulsification curve at low amounts of copolymer is highly different (Fig. 4d). In that case, when adding interfacial modifier, d_v increases up to 2% of copolymer, then decreases while leveling off at 13% of copolymer.

Since the average phase size and the total volume of dispersed phase can be calculated with good precision, the apparent interfacial area occupied per molecule of copolymer (A_{app}) can be estimated [26,40]. This approach assumes that at the critical concentration, all the copolymer has migrated to the interface. Hence, the interfacial area occupied per molecule can be estimated directly from the emulsification curve data (at the critical concentration) using the following equation:

$$A_{app} = (6*Mn*\Phi_D)/(d_v*N_A*\rho_c*\Phi_C) \quad (1)$$

In eq. (1) Φ_D and Φ_C represent the volume fraction of dispersed phase (TPS) and copolymer at C_{crit}, respectively; ρ_D, ρ_C and Mn represent the density of the dispersed phase, the density of the copolymer and the number average molecular weight of the copolymer, respectively; d_v and N_A are the volume-average diameter at C_{crit} and Avogadro's number, respectively. Finally,

$$A_{app} = 1/\sum = (6 * Mn)/(d_v * Na * C_{crit} * \rho_D) \quad (2)$$

where Σ represents the density of copolymer at the interface. The explanation of Eq. (1) is given elsewhere [26]. The values obtained from the emulsification curve data are shown in Table 3. The apparent interfacial areas occupied per molecule (A_{app}) for the blends from this study range from 1.3 to 2.5 nm^2/molecule (corresponding to areal densities of 0.77 to 0.40 molecules/nm^2). In a previous detailed emulsification study on polystyrene/ethylene-propylene blends [28], it was shown that a diblock copolymer occupied 5.6 nm^2/molecule (areal density of 0.18 molecules/nm^2) and a triblock occupied 27 nm^2/molecule (areal density of 0.037 molecules/nm^2) under conditions where all the copolymer is located at the interface. Since graft copolymers have multiple reacting sites, the interfacial area occupied per molecule of graft copolymers should normally be higher than 5 nm^2/molecule for a similar molecular weight system. Thus, these results strongly indicate that either a significant portion of the PE-g-MA graft copolymer is not finding its way to the interface, or multiple grafting does not occur. In previous work [28] it has been shown that the A_{app} value diminishes when the hypothesis of all copolymer macromolecules migrating to the interface is not respected as could be the case in this work. It is also interesting to note that the apparent interfacial density (Σ) of PE-g-MA graft copolymer decreases from TPS24 to TPS36 blends. This latter observation points to a possible interaction between glycerol and the graft copolymer.

Fig. 5, shows the evolution of the TPS particle size polydispersity (dv/dn) as a function of PE-g-MA graft copolymer concentration for blends prepared at various glycerol plasticizer contents. When adding a graft copolymer to the HDPE/TPS blends containing 28, 36 and 40% of glycerol in the TPS, the particle size distribution (dv/dn) starts to increase. This effect is accentuated and the maximum shifts to higher values of copolymer when more glycerol is present in the thermoplastic starch. This behavior is totally contrary to the expected behaviour upon addition of an interfacial modifier and again points to an interaction between the glycerol content in the thermoplastic starch and the PE-g-MA interfacial modifier. Note that no such interaction is observed for the TPS 24 blend system. It will be shown later in the paper that these results can be understood through the notion of a glycerol-rich outer layer surrounding the TPS phase.

3.2. Dynamic mechanical thermal analysis

The dynamic mechanical properties of thermoplastic starch [41–45] and TPS based blends [16,19,46–48] have been studied by several authors. Previous studies have shown that unplasticized starch presents a unique α relaxation at around 50 °C [42,49]. When starch is plasticized with a relatively high level of glycerol, it is shown that the plasticized starch/glycerol system is heterogeneous. A phase separation results in glycerol-rich domains (β relaxation) and starch-rich domains (α relaxation) [43,44,49,50]. Angellier et al. [45] studied the thermo-mechanical properties of thermoplastic waxy-maize starch matrix plasticized with glycerol. They observed both α and β relaxations for E' (storage modulus) and concluded that glycerol-rich domains were included in a continuous amylopectin-rich phase.

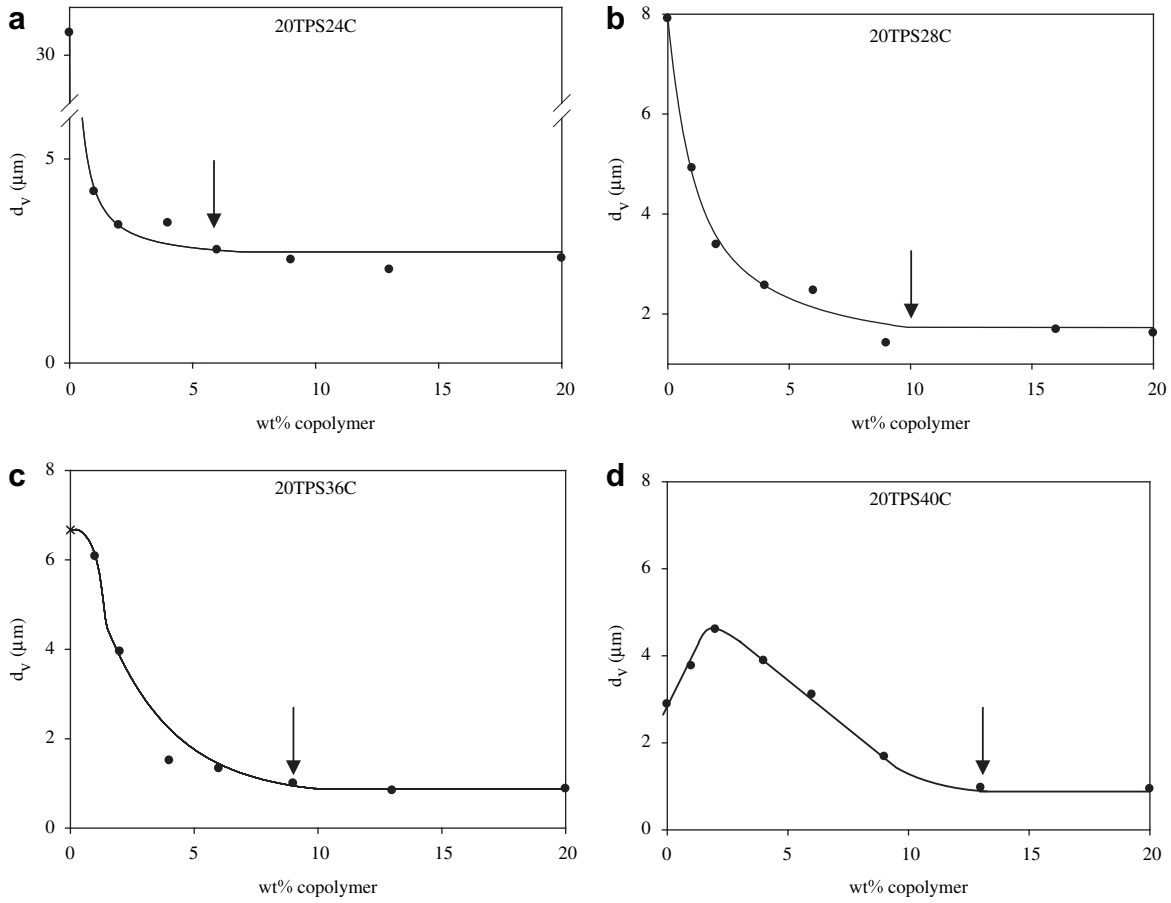

Fig. 4. Influence of the wt % of polyethylene co-maleic anhydride copolymer on the volume-average diameter of the TPS dispersed phase for PE/TPS blends containing: a) TPS24, b) TPS28, c) TPS36 and d) TPS40.

Moreover, they found that the plasticizer content did not influence the relaxation of plasticizer-rich domains, however, the α relaxation occurred at a lower temperature when increasing the glycerol content due to the higher mobility of amylopectin chains (Fig. 6).

In this study the thermograms of the loss modulus of blends containing 20% of TPS24, 28, 36 and 40 containing different amounts of PE-g-MA (Figs. 7–10), exhibit two main peaks. The low temperature peak (T_β) is the secondary relaxation of starch and corresponds to the secondary-transition of glycerol-rich domains, whereas the higher temperature peak (T_α) is the primary-transition of amylopectin rich-domain [43] as discussed above. As shown in Fig. 6, the amplitude of the peak assigned to T_α is somewhat higher at low glycerol contents (20TPS24 and 20TPS28) as compared to 20TPS36 and 20TPS40. This is an indication of the increased mobility of the starch phase with plasticizer content as found by other authors [44,45]. As well, it can be seen that the amplitude of the T_α peak does not vary significantly with the amount of added PE-g-MA (Figs. 7–10).

The T_β peak in the loss modulus curve, on the other hand, shows a more distinct shift to lower temperatures and a significant growth in amplitude when more glycerol is added to the thermoplastic starch (Fig. 6). Secondly, it is clearly shown that T_β increases and the amplitude of the peak decreases when adding PE-g-MA (Figs. 7–10). The precise temperatures of the T_β peaks for compatibilized 20TPS28 and 20TPS36 blends are summarized in Table 4 and it can be seen that a six and seven degree shift respectively is observed over the range of added PE-g-MA concentrations. In fact, the effect of adding PE-g-MA to high glycerol content TPS blends results in T_β peak shifts and amplitude changes very similar to the effect of reducing the glycerol content.

These results clearly point to a TPS phase in polyethylene that is a partially miscible mixture of glycerol and starch. Furthermore, both the position and the amplitude of the glycerol-rich T_β phase, are significantly influenced by added PE-g-MA modifier while the starch-rich phase is affected much less. Thus, as in the emulsification work discussed earlier on in the paper, these results also point to an interaction between the glycerol in the thermoplastic starch and the added PE-g-MA.

Table 3
Critical concentration of copolymer, number, surface and volume-average diameter at C_{crit}, calculated interfacial area occupied per molecule (A_{app}) and interfacial density of copolymer Σ (in copolymer per nm^2) for 20TPS24, 20TPS28, 20TPS36 and 20TPS40 blends.

Blends 20%TPS[a]	C_{crit}, wt%	d_n (at C_{crit}), in µm	d_s; d_v (at C_{crit}), in µm	A_{app}, in nm^2/molecule	Σ, in molecule/nm^2
TPS24	6	1.2	2.1; 2.8	1.3	0.77
TPS28	9	0.71	1.3; 1.7	1.5	0.67
TPS36	9	0.55	0.84; 1.0	2.5	0.40
TPS40	13	0.37	0.64; 0.97	1.8	0.56

[a] The exact glycerol content for each of the TPS samples shown in the Table can be found in the Experimental.

3.3. Reaction between glycerol and anhydride

It is well known that an anhydride moiety can react with an alcohol leading to esterification [34]. To verify if this reaction can occur in the investigated materials, pure glycerol and (2-dodecen-1-yl)succinic anhydride were mixed in an ethanol co-solvent

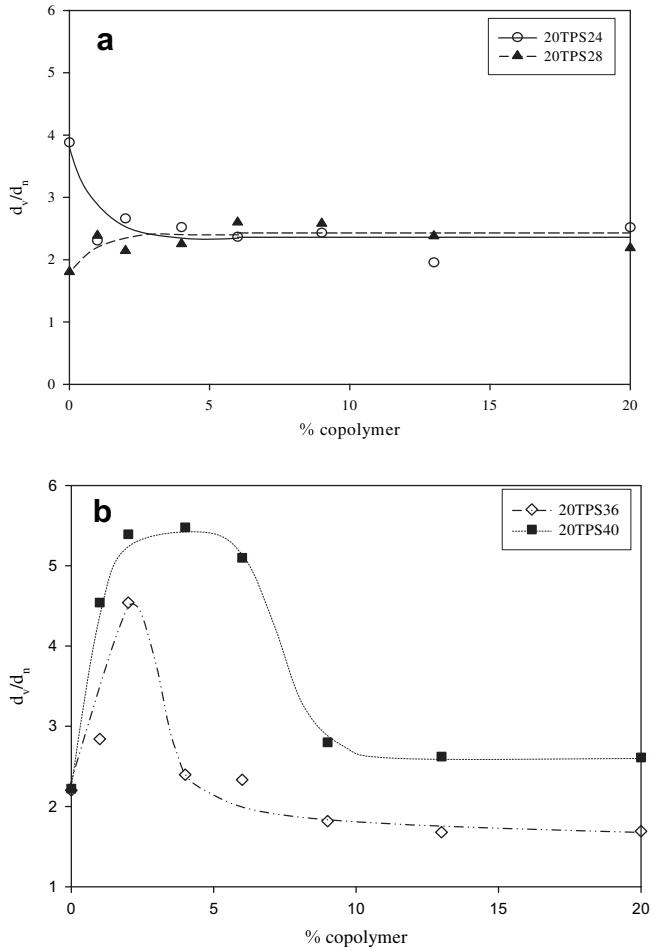

Fig. 5. Polydispersity of the TPS dispersed phase size versus wt% of PE-g-MA copolymer for PE/TPS blends containing a) TPS24 (○), TPS28 (▲); and b) TPS36 (◇) and TPS40 (■).

and reacted for 24 h at 80 °C. The (2-dodecen-1-yl)succinic anhydride exhibits 2 absorption bands at 1784 and 1860 cm^{-1} (spectra not shown) assigned to the symmetric and asymmetric stretching modes of the C═O group, respectively [51–53]. The peaks attributed to the stretching bands of the C–O link are located at 919 and 1229 cm^{-1}. After reaction, the absence of peaks at 1784 and 1860 cm^{-1} prove that the C–C(O)–O–C(O)–C anhydride moieties have disappeared.

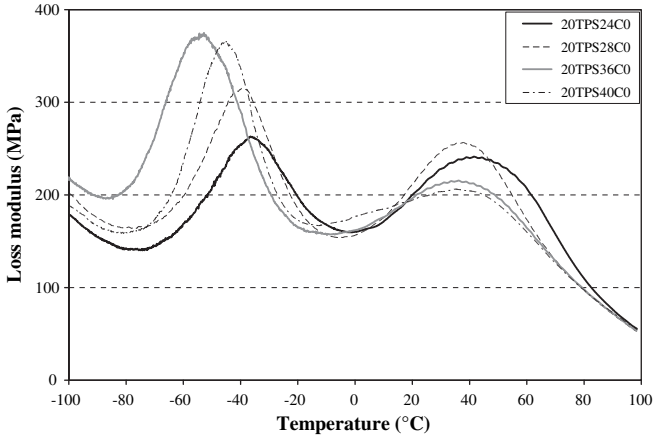

Fig. 6. Loss modulus of unmodified PE/TPS blends containing 24, 28, 36 and 40% of glycerol.

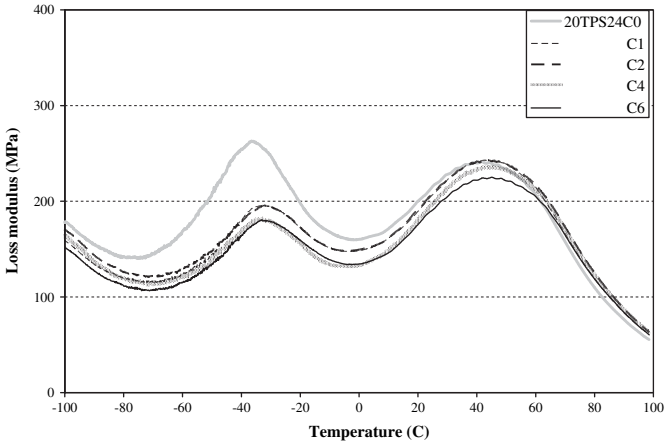

Fig. 7. Loss modulus of different PE/TPS24 blends containing 0, 1, 2, 4 and 6 wt % of PE-g-MA copolymer.

Moreover two peaks centered at 1706 and 1180 cm^{-1} assigned to the C═O and C–O stretching frequency of ester appear. Hence, reaction between glycerol and (2-dodecen-1-yl)succinic anhydride did lead to esterification in these reaction conditions. In the extrusion process, the contact time is much shorter than in this control experiment. However, the intense mixing conditions and high temperature likely provide sufficient conditions to achieve esterification.

3.4. Impact strength

As mentioned in the experimental part, the 20TPS36 and 20TPS40 blends were very ductile materials and even a high energy pendulum (25 J) was not able to break the specimens. Hence, Fig. 11 only reports the impact strength for 20TPS24 and 20TPS28 blends. The under-plasticized blend (20TPS24) exhibits increasing impact strength versus copolymer amounts. In that case, above the critical concentration, the copolymer results in an increase in the energy to break for the samples.

With a more highly plasticized blend (20TPS28), one notices first a drop in the energy to break of the specimen, then an increase up to the critical concentration. In that case, the TPS is sufficiently plasticized and both glycerol and copolymer are responsible for this behaviour, as will be explained later.

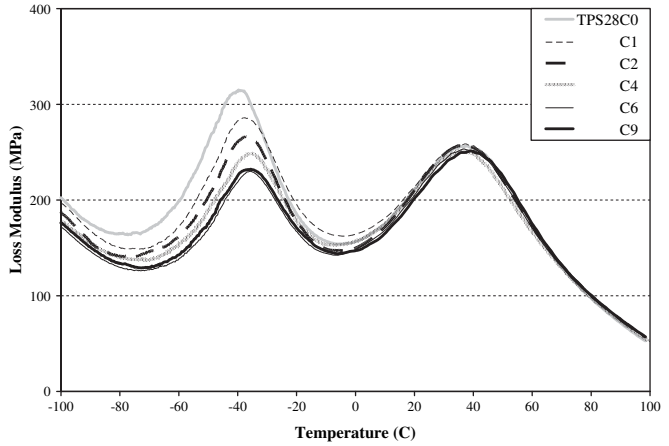

Fig. 8. Loss modulus of different PE/TPS28 blends containing 0, 1, 2, 4, 6 and 9 wt % of PE-g-MA copolymer.

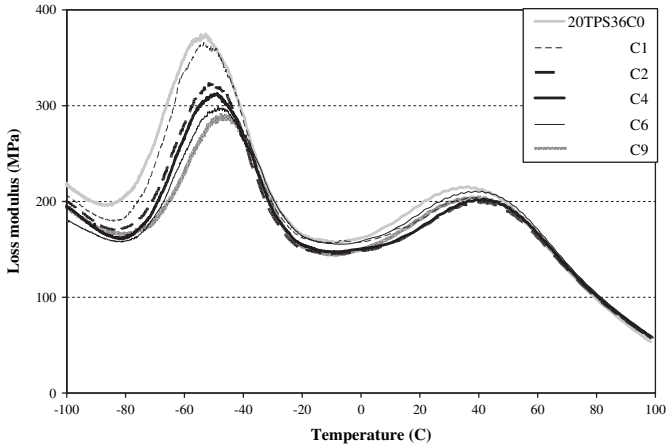

Fig. 9. Loss modulus of different PE/TPS36 blends containing 0, 1, 2, 4, 6 and 9 wt % of PE-g-MA copolymer.

3.5. Tensile properties

The evolution of tensile properties are directly linked with the adhesion between the TPS dispersed phase and the matrix. The elongation at break, ϵ_b, is a high strain property which is particularly sensitive to the state of the interface. Fig. 12a and b shows the evolution of the elongation at break for 20TPS24, 20TPS28, 20TPS36 and 20TPS40 blends with the amount of copolymer. Firstly it is shown in Fig. 12 that the best elongations at break are obtained for 20TPS28 and 20TPS36 blends. The 20TPS24 blend is not sufficiently plasticized even though the emulsification is good and the apparent interfacial density of copolymer is higher than for the other blends. Thus, the TPS24 dispersed phase cannot be sufficiently deformed during the tensile test and elongations are lower than 30%. On the other hand, 20TPS40 blends are overplasticized and the glycerol softens the material.

The 20TPS28 and 20TPS36 blends both possess the highest values of elongation. The behaviour of the elongation at break versus % copolymer curve exhibits three different stages. Firstly, for low amounts of copolymer (1 or 2%), the elongation at break decreases. This drop is more evident in the case of 20TPS28. Then, at 1 or 2%, the elongation starts rising and levels off above C_{crit} (critical concentration for emulsification from Fig. 4).

Table 4
Temperatures of β relaxation for 80PE/20TPS28 and 80PE/20TPS36 blends containing 0, 1, 2, 4, 6, 9 or 13 wt.% of PE-g-MA copolymer.

Wt% of copolymer	T_β (°C)	
	20TPS28 blends	20TPS36 blends
0	−39.7	−53.4
1	−37.4	−53.2
2	−37.4	−50.6
4	−35.2	−48.6
6	−36.0	−47.9
9	−35.6	−47.4
13	−33.9	−46.4

4. Model of a thin glycerol-rich layer at the interface

Up to this point the emulsification curves, the DMTA data and the mechanical properties have pointed to an interaction between the polyethylene-g-MA and the glycerol in the TPS. FTIR clearly indicates the potential of forming ester links through the reaction of the alcohol groups in the glycerol and the anhydride groups in the PE-g-MA. In this section we will attempt to elucidate the nature of that interaction.

The dispersed thermoplastic starch in these PE/TPS blends is, in fact, a heterogeneous partially miscible phase comprised of glycerol-rich and starch-rich regions. Previous studies on other heterogeneous dispersed phase systems have clearly shown a tendency for the low interfacial tension component to migrate and form a thin shell around the dispersed phase [54]. It is thus likely that during melt processing, a small portion of the glycerol-rich phase in the thermoplastic starch may find its way to the thermoplastic starch-polyethylene interface. In fact, such behavior is theoretically supported by the Harkins equation in which the tendency for one phase to separate the two other ones can be estimated by Eq. (3). Eq. (3) is an alternate form of the Harkins equation in which surface tensions were substituted by the appropriate interfacial tensions [55]:

$$\lambda_{31} = \sigma_{12} - \sigma_{32} - \sigma_{13} \tag{3}$$

where σ_{12}, σ_{32} and σ_{13} are the interfacial tensions for each component pair, and λ_{31} is defined as the spreading coefficient for the case of component 3 encapsulating component 1. The index 2 refers to the matrix. λ_{31} must be positive for component 1 to be encapsulated by component 3. This concept was successfully applied by Reignier et al. [56–58] to the case of encapsulation behavior in composite droplet-type HDPE/PS/PMMA blends. When

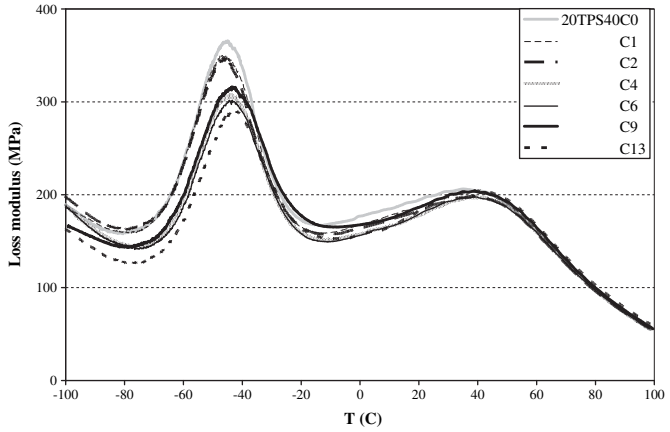

Fig. 10. Loss modulus of different PE/TPS40 blends containing 0, 1, 2, 4, 6, 9 and 13 wt% of PE-g-MA copolymer.

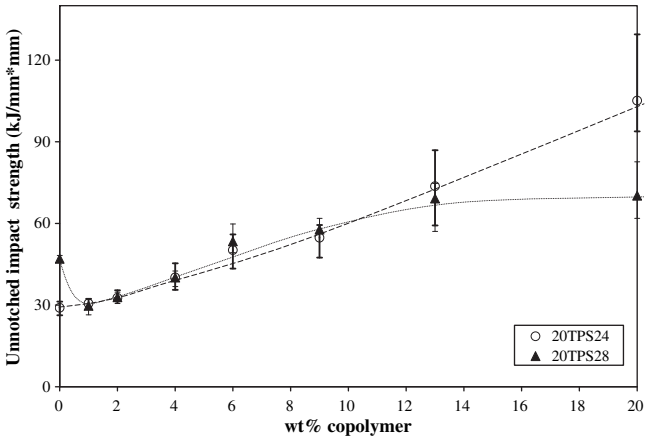

Fig. 11. Impact strength for both PE/TPS24 and PE/TPS28 blends. The curves drawn for the mechanical properties are guides for the eye.

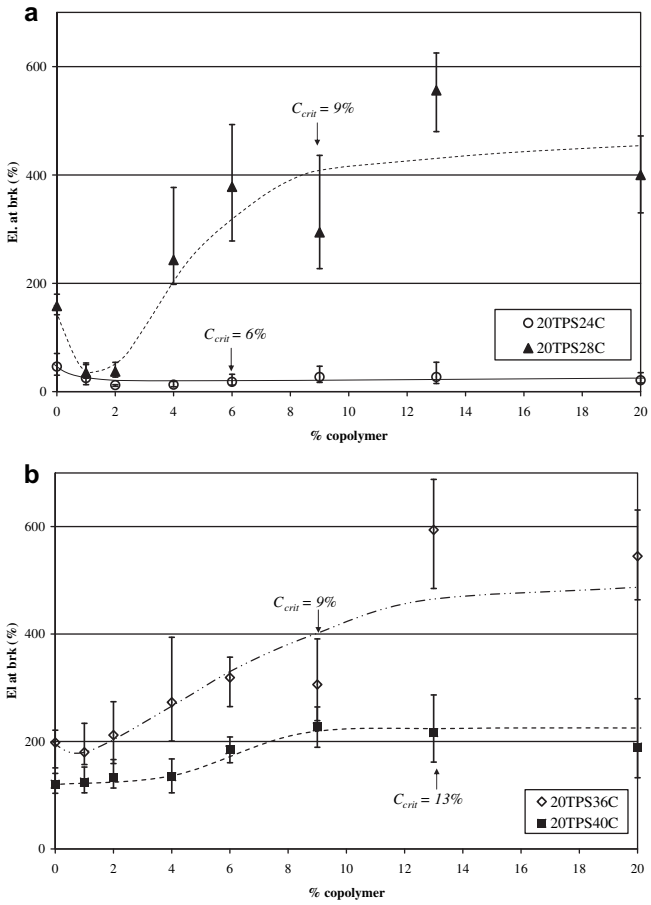

Fig. 12. Elongation at break (in %) versus the wt % of PE-g-MA copolymer for PE/TPS blends containing a) TPS24 (○), TPS28 (▲); and b) TPS36 (◇) and TPS40 (■). The curves drawn for the mechanical properties are guides for the eye. The C_{crit} value is taken from the emulsification curves.

HDPE was the major component, the spreading coefficients predicted a morphology consisting of an HDPE matrix with a PS dispersed phase and PMMA subinclusions within the PS [56]. Shell formation in the case of a low molecular weight glycerol layer in the current system should be significantly easier to achieve than a highly viscous polymer.

In the present case, Eq. (3) can be rewritten as follows in Eq. (4):

$$\lambda_{\text{glycerol/starch}} = \sigma_{\text{starch/HDPE}} - \sigma_{\text{glycerol/HDPE}} - \sigma_{\text{starch/glycerol}} \tag{4}$$

It is well known that interfacial tension depends on molecular weight and that this dependence is particularly pronounced in the lower molecular weight range [59]. This originates from entropic effects [54]. Starch and glycerol have virtually identical surface tensions of 63.7 and 64.0 mJ m^{-2} [60–62], respectively. However they differ significantly in molecular weight. The starch component of TPS is typically reported to have molecular weights of 10^5–10^6 for amylose and 10^7–10^9 for amylopectin while glycerol is a small molecule of 92 g/mol molecular weight. This, of course, represents a dramatic difference in molecular weights and it can be readily assumed that $\sigma_{\text{glycerol/HDPE}}$ will be significantly smaller than $\sigma_{\text{starch/HDPE}}$ and that $\sigma_{\text{starch/glycerol}}$ will be very low as is typical for a partially miscible mixture. Thus, the spreading coefficient $\lambda_{\text{glycerol/starch}}$ must clearly be a highly positive value, particularly since $\sigma_{\text{starch/HDPE}}$ is known to be high [63]. This would lead to the spontaneous formation of a thin glycerol-rich layer during melt mixing at the TPS/polyethylene interface in order to reduce the overall surface free energy of the system. In fact, one can consider this glycerol-rich thin layer as a type of surfactant which reduces the interfacial tension between HDPE and the thermoplastic starch.

Postulating a thin glycerol layer at the interface allows one to explain virtually all of the anomalies presented by this polymer blend system with thermoplastic starch. It is difficult to say just how thin the glycerol layer is, but it is expected to be in the 10–20 nm range. Efforts to characterize this layer have been difficult. This is very similar to the scale level of the interfacial region in modified polymer blends and rigorous analysis and detection of that has also been difficult. The characterization of this layer will be carried out in a separate study.

The high impact strength obtained for 20TPS28C0 and the good elongations at break obtained for all unmodified 20TPS24C0, 20TPS28C0, 20TPS36C0 and 20TPS40C0 blends (as shown in Figs. 11 and 12, respectively) can be explained by this glycerol-rich layer. Indeed, in those blends the stress is transmitted from the matrix to the dispersed phase by a glycerol layer at the interface.

The increase in particle size (Fig. 4d) and particle size distribution (Fig. 5) can also be understood through the presence of a thin glycerol-rich layer at the surface of the thermoplastic starch. This layer would interact directly with the added PE-g-MA and initially impede its interaction with the starch component of the thermoplastic starch. This effect is very pronounced for the 20TPS40 and even for the 20TPS36 blends (Fig 4c and d respectively). The effect diminishes as glycerol content in the TPS drops to TPS28 and TPS24. The decrease in the apparent areal density of copolymer at the

interface with glycerol content (Table 3) would also be expected if the copolymer had more of a tendency to interact with glycerol in 20TPS36 and 20TPS40. The notion of a glycerol-rich outer layer would not be expected to affect the calculation of A_{app} significantly since the glycerol-rich layer is expected to be a very small quantity when compared to the overall volume of TPS in the system (much like an interfacially modified system in classic polymer blends). The calculation requires the estimation of an interfacial area of dispersed phase which will be very largely dominated by the bulk of the thermoplastic starch.

The trends in the DMTA thermograms can also be rationalized through the presence of a glycerol-rich layer at the PE-thermoplastic starch interface. For all TPS based blends (in Figs. 7–10) it is shown that the copolymer affects the glycerol-rich domains, much more than the starch-rich domains, by increasing the temperature and decreasing the amplitude of the T_β peak. Since the copolymer interacts with glycerol from the interface the T_β peak shifts in a fashion similar to an effect of reducing the glycerol content in the blends (see Fig. 6).

This glycerol layer at the interface is idealized in the schematic shown in Fig. 13. For all the uncompatibilized systems, this mechanism can potentially explain the high mechanical properties, particularly the high elongation at break which is normally very closely related to the quality of interfacial interactions. In classical polymer blends, unmodified high interfacial tension systems typically display very poor interfacial interactions. Under such circumstances even a blend of two highly ductile components will display brittle fracture even at low concentrations of minor phase [64–66]. This is principally due to an inability to effectively transfer stress at the interface resulting in the interface becoming the weakest part of the blend system. In this study on PE/TPS, the thin, low molecular weight, interfacial glycerol layer at the interface serves as a type of interfacial modification. When the polyethylene matrix is deformed through the application of stress, the glycerol-rich interfacial layer readily deforms due to its very low molecular weight even though the interfacial tension between glycerol and PE is high. Once the glycerol-rich interfacial layer deforms, stress is effectively transferred to the starch-rich phase and through the entire thermoplastic starch system due to the very high partially miscible interactions between the starch-rich and glycerol-rich phase.

This work, in fact, potentially points to an entirely new strategy to modify interfaces in polymer blends through the use of small molecule modifiers and plasticized polymers.

When PE-g-MA copolymer is further added to the system, a type of double interfacial interaction mechanism comes into play. Initially, the maleic anhydride will react with the interfacial glycerol-rich layer, as demonstrated by FTIR, particularly if the level of glycerol in the TPS is quite high. Evidence of this maleic anhydride-glycerol interaction has been demonstrated above in the emulsification curves, the DMTA data, the mechanical properties and by FTIR. As the glycerol layer thickness decreases, the added copolymer chains also interact with the starch-rich phase and accumulate at the interface. Ultimately, an optimal combination of both added maleic anhydride grafted copolymer as well as some interfacial glycerol-rich phase combine to result in the best possible mechanical properties. Note that maleic anhydride grafted copolymer in lower glycerol content blends (TPS 24), only delivers a fraction of the mechanical property improvement observed for TPS 28 and TPS 36. Furthermore, an overplasticization of the thermoplastic starch (TPS 40) also results in a decrease in mechanical properties likely due to an overly thick interfacial glycerol layer.

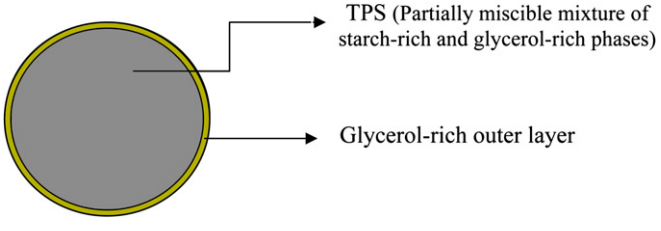

Fig. 13. Schematic representation of a typical TPS particle idealizing the glycerol-rich outer layer.

5. Conclusions

In this study on polyethylene/thermoplastic starch blends, detailed emulsification curves, DMA data and tensile mechanical property results point to the presence of a thin glycerol-rich layer at the PE/TPS interface that serves as a type of interfacial modification. Under dynamic melt-mixing conditions, it is suggested that a small portion of the low molecular weight glycerol-rich phase in the TPS tends to migrate to the HDPE-TPS interface as predicted by the Harkins spreading theory. Once at the interface, this low molecular weight glycerol-rich outer layer is readily deformed by an applied stress and this stress is then transferred to the starch-rich phase due to their mutual partial miscibility. Added PE-g-MA copolymer initially reacts with the glycerol-rich outer layer, but if the level of copolymer is high enough it then reacts with the starch-rich phase via a classic interfacial modification protocol. Ultimately, an optimal combination of both added PE-g-MA copolymer as well as some interfacial glycerol-rich phase combine to result in the best possible mechanical properties. Also, both the elongation at break and impact properties dramatically increase at a copolymer level associated with interfacial saturation. The above mechanism effectively explains all the emulsification and mechanical property observations.

Acknowledgements

The authors gratefully acknowledge the financial support received from the Canadian Biomass Innovation Network and the Natural Sciences and Engineering Research Council of Canada through a Strategic Grant. Appreciation is also extended to Claire Cerclé for valuable comments and input.

References

[1] Russell PL. J Cereal Sci 1987;6(2):133–45.
[2] Willett JL. J Appl Polym Sci 1994;54(11):1685–95.
[3] Chandra R, Rustgi R. Polym Deg Stab 1997;56(2):185–202.
[4] Evangelista RL, Sung W, Jane JL, Gelina RJ, Nikolov ZL. Ind Eng Chem Res 1991;30(8):1841–6.
[5] Sailaja RRN, Chanda M. J Appl Polym Sci 2001;80(6):863–72.
[6] St-Pierre N, Favis BD, Ramsay BA, Ramsay JA, Verhoogt H. Polymer 1997;38(3):647–55.
[7] Favis BD, Rodriguez F, Ramsay BA. Polymer compositions containing thermoplastic starch and process of making. US Patent 6,605,657; 2003.
[8] Rodriguez-Gonzalez FJ, Ramsay BA, Favis BD. Polymer 2003;44(5):1517–26.
[9] Rodriguez-Gonzalez FJ, Virgilio N, Ramsay BA, Favis BD. Adv Polym Tech 2003;22(4):297–305.
[10] Favis BD, Rodriguez Gonzalez FJ, Bruce AR. Method of making polymer compositions containing thermoplastic starch. US Patent 6,844,380; 2005.
[11] Rodriguez Gonzalez FJ. Low density polyethylene/thermoplastic starch blends. PhD thesis; 2002. p. 181.
[12] Sailaja RRN, Reddy AP, Chanda M. Polym Int 2001;50(12):1352–9.
[13] Sailaja RRN. Polym Int 2005;54(2):286–96.
[14] Bikiaris D, Prinos J, Panayiotou C. Polym Deg Stab 1997;56(1):1–9.
[15] Sailaja RRN, Chanda M. J Appl Polym Sci 2002;86(12):3126–34.
[16] Bikiaris D, Panayiotou C. J Appl Polym Sci 1998;70(8):1503–21.
[17] Sailaja RRN, Chanda M. J Polym Mater 2000;17(2):165–76.
[18] Girija BG, Sailaja RRN. J Appl Polym Sci 2006;101(2):1109–20.
[19] Wang S, Yu J, Yu J. Polym Int 2005;54(2):279–85.
[20] Wang N, Yu J, Ma X, Han C. Polym Comp 2007;28(1):89–97.
[21] Huneault MA, Li H. Polymer 2007;48(1):270–80.
[22] Taylor GI. Proc Roy Soc (London) 1932;A138:41–8.

[23] Taylor GI. Proc Roy Soc (London) 1934;A146:501–23.
[24] Favis BD. Polymer 1994;35(7):1552–5.
[25] Israels R, Jasnow D, Balazs AC, Guo L, Krausch G, Sokolov J, et al. J Chem Phys 1995;102(20):8149–57.
[26] Matos M, Favis BD, Lomellini P. Polymer 1995;36(20):3899–907.
[27] Cigana P, Favis BD, Jerome R. J Polym Sci B Polym Phys 1996;34(9):1691–700.
[28] Cigana P, Favis BD. Polymer 1998;39(15):3373–8.
[29] Favis BD, Chalifoux JP. Polym Eng Sci 1987;27(21):1591–600.
[30] Saltikov SA. Proceedings of the second international congress for stereology. Berlin: Springer-Verlag; 1967.
[31] Lepers J-C, Favis BD, Tabar RJ. J Polym Sci B Polym Phys 1997;35(14):2271–80.
[32] Liang H, Favis BD, Yu YS, Eisenberg A. Macromolecules 1999;32(5):1637–42.
[33] Ramkumar DHS, Bhattacharya M, Vaidya UR. Eur Polym J 1997;33(5):729–42.
[34] Bayram G, Yilmazer U, Xanthos M, Patel SH. J Appl Polym Sci 2002;85(12): 2615–23.
[35] Bourry D, Favis BD. Polymer 1998;39(10):1851–6.
[36] Lomellini P, Matos M, Favis BD. Polymer 1996;37(25):5689–94.
[37] Noolandi J, Hong KM. Macromolecules 1982;15(2):482–92.
[38] Noolandi J. Polym Eng Sci 1984;24(2):70–8.
[39] Vilgis TA, Noolandi J. Macromolecules 1990;23(11):2941–7.
[40] Paul DR, Newman S, editors. Polymer blends, vol. 2. New York: Academic Press; 1978. p. 35.
[41] Sala RM, Tomka IA. Angew Makromol Chem 1992;199:45–63.
[42] Lourdin D, Bizot H, Colonna P. J Appl Polym Sci 1997;63(8):1047–53.
[43] Angles MN, Dufresne A. Macromolecules 2000;33(22):8344–53.
[44] Angles MN, Dufresne A. Macromolecules 2001;34(9):2921–31.
[45] Angellier H, Molina-Boisseau S, Dole P, Dufresne A. Biomacromolecules 2006;7(2):531–9.
[46] Averous L, Moro L, Dole P, Fringant C. Polymer 2000;41(11):4157–67.
[47] Averous L, Fauconnier N, Moro L, Fringant C. J Appl Polym Sci 2000;76(7): 1117–28.
[48] Martin O, Averous L. Polymer 2001;42(14):6209–19.
[49] Wilhelm HM, Sierakowski MR, Souza GP, Wypych F. Carbohydr Polymer 2003;52(2):101–10.
[50] Stading M, Rindlav-Westling A, Gatenholm P. Carbohydr Polymer 2001;45(3): 209–17.
[51] Bettini SHP, Agnelli JAM. J Appl Polym Sci 1999;74(2):247–55.
[52] Bettini SHP, Agnelli JAM. Polym Test 1999;19(1):3–15.
[53] Sclavons M, Franquinet P, Carlier V, Verfaillie G, Fallais I, Legras R, et al. Polymer 1999;41(6):1989–99.
[54] Broseta D, Fredrickson GH, Helfand E, Leibler L. Macromolecules 1990;23(1): 132–9.
[55] Hobbs SY, Dekkers MEJ, Watkins WH. J Mater Sci 1988;23(4):1219–24.
[56] Reignier J, Favis BD. Macromolecules 2000;33(19):6998–7008.
[57] Reignier J, Favis BD, Heuzey M-C. Polymer 2002;44(1):49–59.
[58] Reignier J, Favis BD. AIChE J 2003;49(4):1014–23.
[59] Anastasiadis SH, Gancarz I, Koberstein JT. Interfacial tension of immiscible polymer blends: temperature and molecular weight dependence. Storrs, CT, USA.: Univ. Connecticut; 1988. pp. 41.
[60] Bialopiotrowicz T. Food Hydrocolloids 2003;17(2):141–7.
[61] Carvalho AJF, Curvelo AAS, Gandini A. Ind Crop Prod 2005;21(3):331–6.
[62] Karbowiak T, Debeaufort F, Voilley A. Crit Rev Food Sci Nutr 2006;46(5): 391–407.
[63] Biresaw G, Carriere CJ. J Polym Sci B Polym Phys 2001;39:920–30.
[64] Narisawa I, Ishikawa M, Ogawa H. J Mater Sci 1980;15(8):2059–65.
[65] Ishikawa M, Narisawa I. J Mater Sci 1983;18(7):1947–57.
[66] Kinloch AJ, Young RJ. Fracture behaviour of polymers. New York: Applied Science Publishers; 1983.